Variational Mode-Matching: An Advanced Simulation Method for Guided-Wave Photonic Devices

N. Finger[†], C. Pacher, and W. Boxleitner

ARC Seibersdorf research GmbH (ARC-sr), Donau-City-Str. 1, 1220 Vienna, Austria

***Abstract*— We present a novel method — the variational mode-matching (VMM) method — for the simulation of planar-waveguide based photonic devices for, e.g., wavelength filter and input/output coupler applications. These devices may contain quasi-periodic grating couplers, waveguide transitions, and tapers. VMM preserves the advantages of film mode-matching (MM) techniques while increasing the robustness and providing the capability of adaptive refinement for fast convergence. To demonstrate the efficiency of this approach, two grating-based devices showing strong coupling with radiation fields are investigated numerically.**

I. Introduction

The in-depth simulation of wave-propagation phenomena in complex guided-wave multi-section devices like grating-based wavelength filters or input/output couplers employing strongly coupling gratings such as surface gratings and/or showing abrupt waveguide transitions requires rigorous numerical methods. Among these methods are mode-matching (MM) techniques [1][2] which must be combined with perfectly-matched layers (PMLs) [3] to permit an accurate description of radiation fields. However, MM can only be as stable as the algorithms which are used to determine the spectrum of the local PML waveguide modes. Since the proper classification of PML modes is often very difficult, instabilities can arise from an improper truncation of the mode spectrum. In addition, MM only allows uniform refinement as the number of modes in the field expansion is increased what may lead to rather slow convergence and, thus, a significant numerical overhead.

In the following, the VMM method preserving the advantages of MM while avoiding the drawbacks mentioned above will be presented.

II. Theory

With the 2D-assumption $\partial_y(\cdot) = 0$ Maxwell's equations for dielectric materials characterized by the dielectric permittivity $\varepsilon(x, z)$ take the form

$$\partial_x a \partial_x \phi + \partial_z a \partial_z \phi + k_0^2 b\phi = \imath k_0 j_0(x)\delta(z - z_S) \qquad (1)$$

where $\phi = E_y$, $a = 1$, $b = \varepsilon$ for TE- and $\phi = H_y$, $a = \frac{1}{\varepsilon}$, $b = 1$ for TM-polarization, respectively; $k_0 = \frac{2\pi}{\lambda_0}$ (vacuum wavelength λ_0). In the z-direction, the simulation domain $0 \le z \le L$ is assumed to be terminated by either electric or magnetic walls. To mimic an open domain, PMLs are introduced via complex variable stretching [3]: $z \mapsto z + \imath \int_0^z \mathrm{d}\tau\, \sigma(\tau)$ at the boundaries. For incoupling problems an equivalent driving current $j_0(x)$ located at $z = z_S$ is assumed causing the incident field $\phi^{(\mathrm{in})}(x, z_S)$.

To solve the homogeneous problem for a layered system, the separation ansatz

$$\phi(x, z) = \sum_{j=1}^{n_\varphi} \psi_j(x)\varphi_j(z) \qquad (2)$$

with transverse shape functions $\varphi_j(z)$, which must fullfill the outer boundary conditions (Dirichlet or Neumann), is used. Apart from this constraint, the set of shape functions may be chosen rather freely offering the opportunity of adaptive refinement in z-regions where rapid variations of the field are expected (e.g., in the grating region of metal gratings).

Within the layer $l = 1, \ldots, n_l$, $x_{l-1} < x < x_l (= x_{l-1} + d_l)$, where ε does not depend on x, the fields $\psi_j(x)$ are of the form

$$\psi_j^{(l)}(x) = \sum_\rho C_{j\rho}^{(l)} \left[A_\rho^{(l)} \mathrm{e}^{\imath\beta_\rho^{(l)}(x - x_{l-1})} + B_\rho^{(l)} \mathrm{e}^{-\imath\beta_\rho^{(l)}(x - x_l)} \right] \qquad (3)$$

where the (approximate) modal propagation constants $\beta_\rho^{(l)}$ and modal expansion coefficients $C_{j\rho}^{(l)}$ are obtained from the eigenvalue problem $\mathbf{E}^{(l)}\vec{C}_\rho^{(l)} = (\beta_\rho^{(l)}/k_0)^2 \mathbf{V}^{(l)}\vec{C}_\rho^{(l)}$ with $(\mathbf{V}^{(l)})_{mj} = \int \mathrm{d}z\, \varphi_m(z) a^{(l)}(z)\varphi_j(z)$ and $(\mathbf{E}^{(l)})_{mj} = \int \mathrm{d}z\, \varphi_m(z) b^{(l)}(z)\varphi_j(z) - \frac{1}{k_0^2}\int \mathrm{d}z\, (\partial_z\varphi_m(z)) a^{(l)}(z)(\partial_z\varphi_j(z))$. To determine the A- and B-coefficients in (3) the continuity of ϕ and $\frac{1}{\imath k_0} a\partial_x\phi$ across the x-interfaces is exploited yielding the layer-to-layer scattering matrix

$$\begin{bmatrix} \mathbf{t}^{(l)}\vec{A}^{(l)} \\ \mathbf{t}^{(l+1)}\vec{B}^{(l+1)} \end{bmatrix} = \begin{bmatrix} \hat{\mathbf{R}}_{l,l+1} & \hat{\mathbf{T}}_{l,l+1} \\ \hat{\mathbf{T}}_{l+1,l} & \hat{\mathbf{R}}_{l+1,l} \end{bmatrix} \begin{bmatrix} \vec{B}^{(l)} \\ \vec{A}^{(l+1)} \end{bmatrix} \qquad (4)$$

where

$$\begin{bmatrix} \hat{\mathbf{R}}_{l,l+1} & \hat{\mathbf{T}}_{l,l+1} \\ \hat{\mathbf{T}}_{l+1,l} & \hat{\mathbf{R}}_{l+1,l} \end{bmatrix} = \begin{bmatrix} \mathbf{C}^{(l)} & -\mathbf{C}^{(l+1)} \\ \mathbf{D}^{(l)} & \mathbf{D}^{(l+1)} \end{bmatrix}^{-1} \begin{bmatrix} -\mathbf{C}^{(l)} & \mathbf{C}^{(l+1)} \\ \mathbf{D}^{(l)} & \mathbf{D}^{(l+1)} \end{bmatrix}$$

with $\mathbf{t}^{(l)} = \mathrm{diag}(\mathrm{e}^{\imath\beta_\rho^{(l)} d_l})$ and $\mathbf{D}^{(l)} = \mathbf{V}^{(l)}\mathbf{C}^{(l)}\mathrm{diag}(\beta_\rho^{(l)}/k_0)$. This scattering-matrix scheme establishes a numerically stable method for modeling multilayer systems [4]. The numerical complexity is $\mathcal{O}(n_l n_\varphi^2)$; calculating the approximate eigenmodes requires additional $\mathcal{O}(n_l' n_\varphi^3)$ flops (n_l': number of *different* local waveguides).

III. Results

To show the effectiveness of the VMM method, we have simulated two waveguide-grating structures (WGSs) based on a SiO/SiN/Air waveguide (SiN layer thickness: $0.5\,\mu$m) with a rectangular surface relief grating with depth h and a duty cycle of 0.5. In the simulation, the WGS is placed between electric walls (to discretize the local waveguide modes) and PMLs. The refractive indices $\sqrt{\varepsilon}$ of SiN and SiO at $\lambda_0 \approx 1.5\,\mu$m have been taken to be 2 and 1.45, respectively. In both examples the $n_\varphi = 100$ lowest order modal fields of the SiO/SiN/Air waveguide with the PMLs turned off (to enhance

[†]e-mail: norman.finger@arcs.ac.at

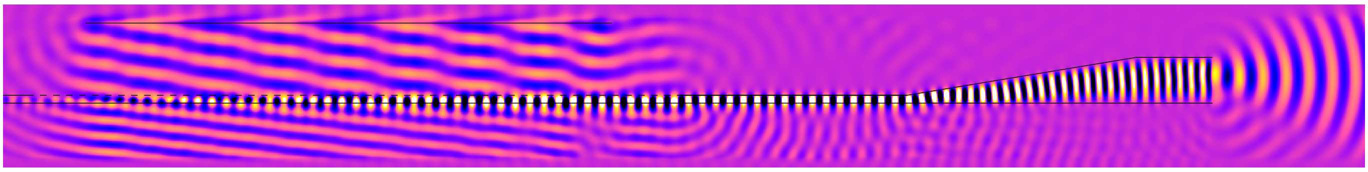

Fig. 3. Optical field in a grating incoupler/taper device with butt-coupling into the air. The taper is approximated by a staircase curve with 25 steps.

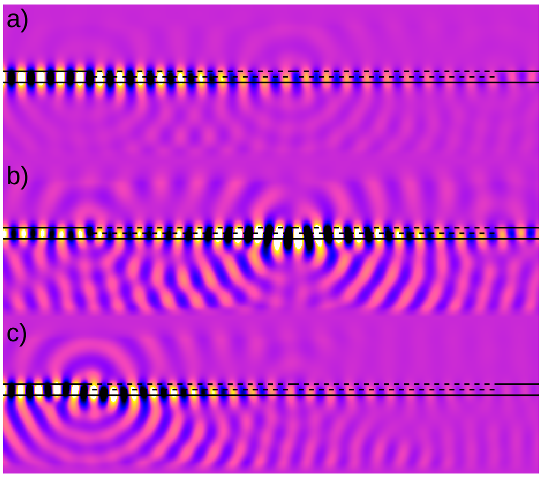

Fig. 1. Field distribution at a) $\lambda_0 = 1.56\,\mu\mathrm{m}$ (right SB edge), b) $\lambda_0 = 1.5215\,\mu\mathrm{m}$ (localized defect mode), c) $\lambda_0 = 1.46\,\mu\mathrm{m}$ (left SB edge).

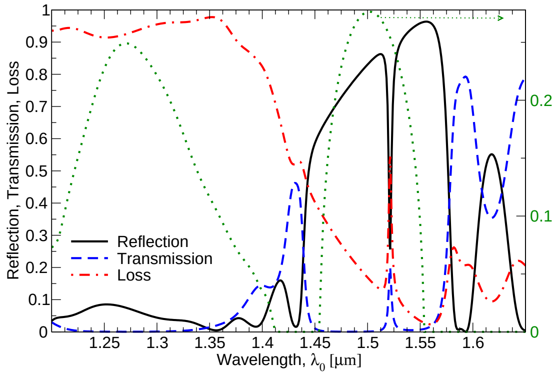

Fig. 2. Left axis: Power reflection, transmission and radiation losses in a finite-length WGS (40 periods) with phase shift. Right axis: Amplitude attenuation in the infinite grating.

the convergence rate of the series (2)) have been used as ansatz functions. Notice that the PMLs enter the model via the matrices $\mathbf{V}^{(l)}$ and $\mathbf{E}^{(l)}$ rigorously.

The first structure comprises a finite-length WGS ($h = 0.25\,\mu\mathrm{m}$, grating period $p = 0.45\,\mu\mathrm{m}$, 40 periods) with a $\approx \frac{\lambda_n}{4}$-phase shift in the middle (see sketch in Fig. 1). The fundamental TE mode is assumed to be incident from the left. Fig. 2 depicts the power reflection, transmission and radiation losses as well as the modal amplitude attenuation for an infinite (i.e., strictly periodic) WGS, which has been obtained from a Floquet-Bloch theory [5], as a function of the wavelength. The broadening of the stopband (SB) compared to that one occurring in the infinite WGS can mainly be attributed to the phase-shift. In the finite-length structure significant radiation losses occur also well above the onset for grating coupled radiation at $\lambda_0 = 1.41\,\mu\mathrm{m}$. The breakaway of the left (= short-wavelength) SB edge is caused by excessive radiation losses occurring at the interface between the flat waveguide region and the grating region: The standing-wave pattern in the grating region has its antinodes in the low-index grating grooves resulting in a shift of the optical field towards the substrate. This leads to a quite large mismatch of the optical fields and, consequently, to a significant radiation loss. At the right SB edge the standing-wave pattern is concentrated in the high-index grating peaks causing a much smaller mismatch and less radiation loss. The localized defect-mode at $\lambda_0 = 1.5215\,\mu\mathrm{m}$ is strongly damped due to radiation fields excited in the phase-shift region. The findings described above are made evident by the representation of the optical field in Fig. 1.

The second structure is a grating incoupler with 50 periods ($h = 0.125\,\mu\mathrm{m}$, $p = 0.85\,\mu\mathrm{m}$) combined with a linear taper with a length of $15\,\mu\mathrm{m}$ expanding the SiN core from $0.5\,\mu\mathrm{m}$ to $3\,\mu\mathrm{m}$ for butt-outcoupling into the air. 40 grating periods are illuminated with a plane TM-polarized wave with unity amplitude, $\lambda_0 = 1.5\,\mu\mathrm{m}$, and an angle of incidence $\theta = -10.25°$ giving $j_0(x) = 2\cos\theta \mathrm{e}^{\imath k_0 x \sin\theta}$ in (1). The power conversion ratio from the incident plane wave into the TM_0 waveguide mode ($\beta_{\mathrm{TM}_0}/k_0 = 1.6655$) is $25.5\,\%$. Scattering losses at the interfaces between the grating region and the homogeneous waveguide regions are of minor importance due to the rather shallow surface grating. Fig. 3 shows the optical field.

The VMM model of this structure contains 25200 unknowns. The computation time with a not yet optimized implementation in `octave` (a freeware clone of `Matlab`) is about $2\,\mathrm{min}$ on a conventional PC with a $2.66\,\mathrm{GHz}$ CPU. There is still room for improvement by a factor of ≥ 10. A finite-element (FE) model would require about five times more unknowns — assuming a moderate discretization with 10 nodes per λ_n. Since in the VMM model the fields are expanded in terms of very good approximations to the local waveguide modes, phase-errors over long propagation distances (i.e., several hundreds of λ_n's) are not a matter of fact as in a FE discretization.

References

[1] A. S. Sudbo, "Film mode matching: a versatile numerical method for vector mode field calculations in dielectric waveguides," *Pure and Appl. Optics*, vol. 2, pp. 211–233, 1993.

[2] O. P. Franza and W. C. Chew, "Recursive mode matching method for multiple waveguide junction modeling," *IEEE Transaction Micro. Theory Tech.*, vol. 44, pp. 87–92, 1996.

[3] F. L. Teixeira and W. C. Chew, "General closed-form PML constitutive tensors to match arbitrary bianisotropic and dispersive linear media," *IEEE Microwave Guided Wave Lett.*, vol. 8, pp. 223–225, 1998.

[4] L. Li, "Comparison of two recursive matrix algorithms for modeling layered diffraction gratings," *J. Opt. Soc. Am. A*, vol. 13, pp. 1024–1035, 1996.

[5] N. Finger and E. Gornik, "Analysis of metallized-grating coupled twin-waveguide structures," *IEEE J. Quantum Electron.*, vol. 35, pp. 832–843, 1999.